NATIONAL ADVISORY COMMITTEE FOR AERONAUTICS

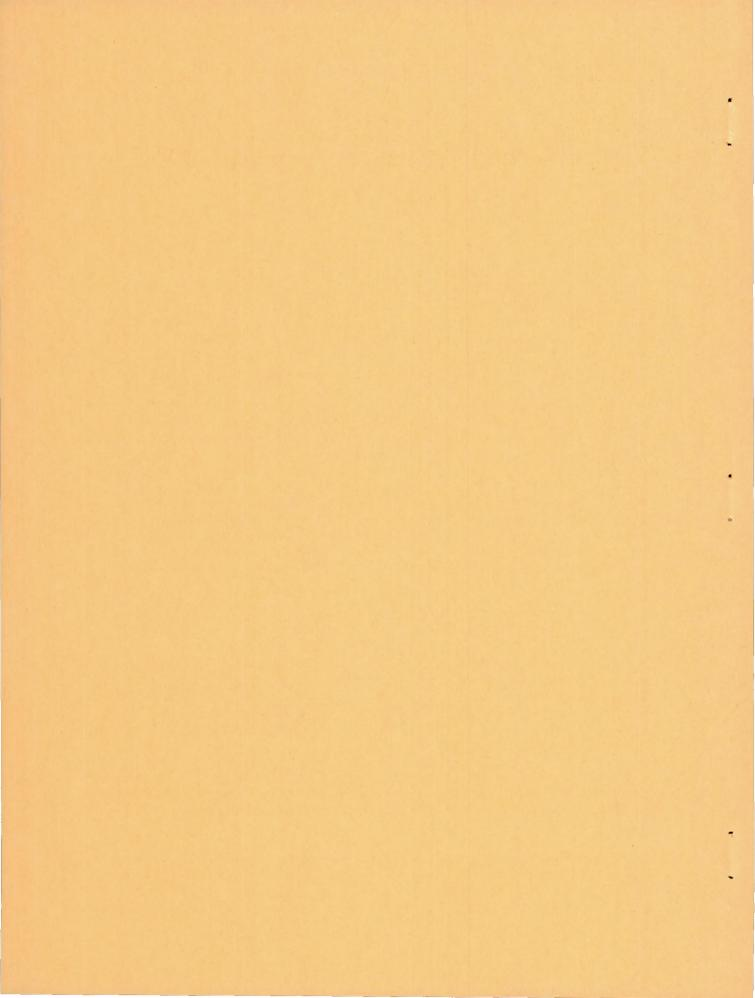
TECHNICAL NOTE 3685

FATIGUE CRACK PROPAGATION IN SEVERELY NOTCHED BARS

By W. S. Hyler, E. D. Abraham, and H. J. Grover
Battelle Memorial Institute



Washington June 1956



NATIONAL ADVISORY COMMITTEE FOR AERONAUTICS

TECHNICAL NOTE 3685

FATIGUE CRACK PROPAGATION IN SEVERELY NOTCHED BARS

By W. S. Hyler, E. D. Abraham, and H. J. Grover

SUMMARY

Fatigue tests were made in rotating bending on severely notched bars machined from 2024-T4 aluminum-alloy extruded round rods. Two sizes of specimens were studied, 1/4-inch-diameter and 2-inch-diameter specimens. The smaller specimens were notched with a V-groove and had notch severities K_t of 5.2. The larger specimens also contained V-grooves with notch severities $K_t = 5.2$ and 13.9.

It was found that, unlike behavior sometimes observed for unnotched and mildly notched bars, fatigue cracks initiated early in the lifetime of the severely notched specimens. In the case of the 1/4-inch-diameter bars, initiation occurred (at a test stress of 22.5 ksi) in less than 0.25 percent of the average lifetime of the specimen.

It appeared that cracks in large-diameter specimens had a period of rapid crack growth followed by a marked tapering off in rate of crack propagation. This behavior may have been associated with compressive residual stresses, which were demonstrated qualitatively to be present. Other factors also may have influenced this behavior.

INTRODUCTION

Considerable study has been given to the growth of fatigue cracks in small unnotched and mildly notched bars (for example, refs. 1 to 4). The evidence available suggests that such cracks form after an appreciable percentage of lifetime at a given stress and propagate slowly at first. At some stage, acceleration of crack growth occurs, which finally terminates in failure of the specimen.

Such studies on severely notched bars have been limited in extent (ref. 5). However, reference 5 shows that fatigue cracks were formed early in the lifetime of specimens that were tested near the fatigue limit.

This investigation was initiated as a notch-size-effect program on 2024-T4 aluminum alloy; however, as a result of the first series of tests

2 NACA TN 3685

on large-diameter severely notched bars, the emphasis of the program was shifted toward a limited study of crack initiation and propagation. The results of the study are presented and discussed in this report.

The program was conducted at Battelle Memorial Institute under the sponsorship and with the financial assistance of the National Advisory Committee for Aeronautics.

MATERIAL

The material used in this investigation was 3-inch-diameter extruded 2024-T4 aluminum alloy. It was purchased by the NACA from the Aluminum Company of America and consisted of bars from one heat cut to approximately 11-foot lengths. As discussed in the appendix, a number of bars were examined using ultrasonic methods to screen out material containing metallurgical defects such as porosity and inclusions.

Following such inspection, standard 0.505-inch-diameter tensile specimens were sectioned from a number of the bars. The locations of these specimens with respect to the cross section of the bar were (1) along the axis of the bar, and (2) along an axis parallel to the bar axis but displaced radially 1 inch. This latter axis location coincided with the minimum section diameter of the large notched bars. The area from which these specimens were taken corresponded generally to the area from which 1/4-inch-diameter specimens were sectioned.

Tensile tests were made in a Baldwin-Southwark universal testing machine equipped with an autographic load-strain recorder. Strain gages were used on two specimens for more accurate determination of the modulus of elasticity. The results of the tests are presented in table I. Average mechanical properties obtained on specimens sectioned from seven bars are as follows:

Location of specimen	Ultimate strength, ksi	Yield strength, ksi	Reduction of area, percent	Modulus of elasticity, psi
Center of bar	72.4	50.3	12.7	107
l inch off center of bar	65.8	45.1	15.3	107

NACA IN 3685

It is apparent that some slight difference in mechanical properties exists over the cross section of the rods. This difference probably is associated with the amount of working or the degree of recrystallization over the cross section.

SPECIMENS

The specimens were notched with V-grooves with root diameters of 1/4 inch or 2 inches. Specimens were sectioned from the 3-inch-diameter round bars as shown in figure 1. Note that the 1/4-inch-diameter specimens were sectioned so that the axis of the specimens passed through a circle 2 inches in diameter (equivalent to the large-specimen minimum diameter).

Four types of specimens were tested. These consisted of unnotched 1/4-inch-diameter specimens, notched 1/4-inch-diameter specimens, and notched 2-inch-diameter specimens with two notch severities. Notch dimensions were such that they covered a wide range of root radii and notch severity. On the basis of information in reference 6, the following listing is a complete description of notched specimen details:

Minimum section diameter, in.	Notch depth, in.	Root radius, in.	Flank angle, deg.	Kt	Kn
0.25	0.031	0.002	60	5.2	2.0
2.00	.25	.002	60	13.9	4.1
2.00	.25	.016	60	5.2	3.0

where

Kn

Neuber's technical stress-concentration factor, $1 + (K_t - 1)/(1 + \sqrt{\rho'/r})$ (ref. 6)

and where

r

notch radius

PI

Neuber's material constant, assumed to be 0.02

In the derivation of K_n , the flank angle ω is assumed to be zero. Other details of the test specimens are shown in figure 2.

Machining of all specimens was carried out on a lathe. Unnotched specimens were rough machined to a dimension about 0.010 inch oversize. This was followed by two finer cuts which removed about 0.006 inch and 0.004 inch successively. Following machining, the unnotched specimens were carefully polished in a special polishing machine. The procedure involved the use, successively, of polishing belts of 240 grit, 400 grit, and 600 grit. The finer the grit size, the less material removed so that about 0.0006 inch of material was polished off with the 600-grit belt. At the conclusion of the polishing operation, polishing scratches ran nearly longitudinal to the specimen axis. Surface roughness was in the range 2 to 5 microinches root mean square.

Notches were machined using a ground-to-shape cutting tool. The procedure for machining the 1/4-inch-diameter specimens was to feed the cutting tool slowly into the specimen to the appropriate depth. The crossfeed mechanism was stopped and the specimen was turned 1 revolution; the cutting tool then was backed off. Cutting oil was used during the machining operation. The specimens were turned at 18 rpm. Crossfeed was set at about 0.0023 inch per specimen revolution. Each specimen was checked for notch depth and contour on a 50:1 shadowgraph. The notches were not polished after completion of machining.

A similar procedure was adopted for the large-diameter specimens. The only departure was that after the crossfeed mechanism was stopped, the specimen turned slowly until the spiral chip broke free. The cutting tool then was backed off. This expedient was adopted to prevent tool chatter at the root of the notch.

MACHINES

Fatigue tests were carried out on two kinds of rotating-beam machines. The R. R. Moore machine was used to test the 1/4-inch-diameter specimens. This machine imposed pure bending on the specimens and was operated at about 10,000 cpm.

The 2-inch-diameter specimens were tested in a Krouse rotating cantilever-beam machine, having a capacity of 60,000 inch-pounds of bending moment. It was operated at about 1,750 cpm.

These machines differ in type of loading and in speed. However, previous experience has not shown these differences to be significant in this type of fatigue test.

EXPERIMENTAL PROGRAM

Preliminary Study of 1/4-Inch-Diameter Specimens

Initial fatigue tests on 1/4-inch-diameter specimens were run to block out S-N curves for unnotched specimens and notched specimens ($K_t = 5.2$, r = 0.002 inch). Data obtained on the initial tests are listed in table II and are shown in figure 3.

Estimated fatigue limits at 10^7 cycles of unnotched specimens and of notched specimens were 24.5 ksi and 17.0 ksi, respectively. The fatigue notch factor K_f computed from these values was 1.45 which was somewhat lower than anticipated.

Preliminary Study of 2-Inch-Diameter Specimens

Prior to continuing further work on small-diameter specimens, the behavior of large-diameter notched specimens was explored. The first large specimen (B-2) tested in rotating bending had a notch with $K_t = 5.2$. The test stress was 22.5 ksi, which according to figure 3 was believed sufficiently high to provide failure in less than 10^6 cycles.

At about 5×10^6 cycles, the test was stopped to examine the notch root. Considerable debris was observed at the notch root and also direct evidence of a gaping crack. The notch root was photographed and the specimen was sectioned and examined metallographically. Figures 4 and 5 show the nature of the notch root after about 5×10^6 cycles of reversed 22.5-ksi stress. The following observations summarize essential details of the three photographs:

- (1) Two almost continuous cracks traverse the notch root circumferentially.
- (2) Occasional areas exist at the notch root from which large pieces of material appear to have fallen out.
- (3) Fatigue cracks initiated on the surface some distance away from the minimum section diameter.
- (4) Propagation of the cracks was toward the center of the bar and in some cases was such that cracks joined, enabling material between the cracks to fall out.
- (5) As a result of deformation during cyclic stressing the contour of the notch root was changed from circular to U-shaped as shown in figures 5(a) and 5(b).

6 NACA IN 3685

The depth of crack penetration was found to be in the range 0.040 to 0.044 inch. The average crack depth (from two measurements) was 0.042 inch.

Factors which might relate to the apparently nonpropagating or slowly propagating crack were considered. The fatigue machine is a constant-load machine. Therefore, if a crack is formed, it should propagate to failure unless metallurgical or other effects inhibit crack growth.

It was thought that extreme fibering of structure might produce the observed behavior. However, examination of a typical section of the structure yielded no proof of such a markedly fibered material. Other metallographic study (for example, hardness measurements) did not disclose positive reasons for observed behavior. Figure 6 shows Knoop hardness numbers taken at various locations on the section observed in figure 4. No trend in hardness gradient was observed in any direction.

Since notches were not polished after machining, there was the possibility that residual machining stresses might have influenced results. A second specimen was tested under identical stress conditions to a lifetime of about 8×10^6 cycles. Failure did not occur; however, severe cracking was present. The notch was remachined and polished with a rotating copper wire (abrasive was FFFF Turkish emery dust in kerosene oil). The specimen was retested and survived about 9×10^6 cycles. A noticeable crack again was in evidence. The specimen then was tested to failure at 27.5 ksi.

The single experiment suggested that machining stresses may not have played a significant role in the observed behavior of the large notched specimen.

Other residual stresses may be more important. Such stresses may arise from heat treatment and aging and may be effective over a more general area of the round bar. Accordingly, a simple residual-stress study was made to determine qualitatively the existence of such gross stress patterns.

The experiment involved sectioning two extruded rods (one, 3 inches in diameter; the other, lathe turned to 2 inches in diameter) with a bandsaw along a diametral plane. Diameter measurements were taken at the end of the specimen at which the saw cut was initiated. In both

NACA TN 3685

cases, the saw cut closed up when the cut was 2 or 3 diameters in length. Data obtained are as follows:

3-inc	h-diameter	specimen	2-inc	h-diameter	specimen
Depth of cut, in.	Diameter, in.	Change in diameter, in.	Depth of cut, in.	Diameter, in.	Change in diameter, in.
0 1 2 3 4 5	2.997 2.993 2.984 2.972 2.957 2.943	0 004 013 025 040 054	0 1 2 3 4 5 6	2.000 1.998 1.993 1.986 1.975 1.963 1.948	0 002 007 014 025 037 052

These values suggest that compressive residual stresses of appreciable magnitude are at the surface of the 3-inch round rod and also at a depth equivalent to the notch-root diameter.

With such stresses, it is possible that propagation of fatigue cracks might be stopped or slowed down. The difference in behavior of large-diameter notched bars and small-diameter notched bars might reflect nearly complete relaxation of stress in the small bars as a result of sectioning. On the basis of these observations, it was thought that continuation of the original program might provide data not readily generalizable to notch-size effect. Accordingly, it was decided to study, on a limited scale, crack propagation in the large and small notched bars.

Study of 1/4-Inch-Diameter Notched Specimens

Crack-propagation studies of 1/4-inch-diameter notched specimens were carried out chiefly at two stress levels, 22.5 ksi and 35.0 ksi. It was thought possible to detect "first cracking" by visual examination under low-power magnification of the notch root while the specimen was under some nominal load less than the test load. While such a technique was helpful in detecting the early stages of cracking, it was not a particularly sensitive procedure (for a notched specimen with an 0.002-inch root radius). The actual method used was merely that of running a specimen to some predetermined lifetime, sectioning the specimen, and measuring the depth of crack penetration. In general, crack depth was determined on four cross sections for each specimen.

8 NACA IN 3685

Data obtained from this study are presented in table III. Included in the table for each specimen are number of cycles of stress and crack-depth measurements on the four sections. The last column in the table contains the average crack depths. It is of interest to note that the two specimens tested at 20.0 ksi which survived more than 10,000,000 cycles had fatigue cracks on the order of 0.004 inch deep. Two other specimens tested at this stress failed in less than 5,000,000 cycles. This suggests that, had the former tests been continued, the cracks might have caused failure.

Data on specimens tested at 22.5 ksi and at 35.0 ksi are plotted in figure 7. The points represent the average crack depth obtained generally from four measurements on each specimen. At the top of the graph, roughly corresponding to the radius of the specimen, are indicated the estimated failure ranges of specimens tested at each stress level. Also indicated in the figure are bands to represent the scatter in crack-depth—lifetime observations.

A number of comments can be made concerning the plotted data as follows:

- (1) At 22.5 ksi, fatigue cracks apparently developed at lifetimes in the range 100 to 1,000 cycles, although failure lifetimes were considerably greater than this lifetime range.
 - (2) At 35.0 ksi, cracks may have been present in less than 100 cycles.
- (3) Propagation of the crack at 22.5 ksi apparently is quite slow over an appreciable portion of the lifetime. At some stage, however, acceleration of crack growth takes place. Final failure may occur in an apparently small percentage of total lifetime. The evidence for this statement is scarce; however, in deliberate attempts to obtain specimens having appreciable crack depth, either failure occurred or the crack depth generally was less than 0.005 inch.
- (4) At 35.0 ksi, the transition between slow propagation and fast propagation may have been less marked. A number of specimens were found which contained cracks of appreciable depth.
- (5) Failure data at a particular stress level usually show appreciable scatter. The experimental evidence suggests that such scatter also is evident in crack initiation and in crack propagation. Since failure is dependent both on initiation and propagation of a crack, the scatter in failure data must reflect on factors associated with crack initiation and with crack propagation.

Study of 2-Inch-Diameter Notched Specimens

Crack propagation studies of the larger size notched specimens were carried out at 22.5 ksi. A few additional fatigue tests were carried out at higher stresses to compare failure data with those of smaller diameter notched specimens. Results are plotted in figure 8. The limited data suggest that specimens with notches of both severities were behaving similarly.

Visual observation of initial cracking also was attempted with about the same degree of success as with small specimens. Therefore, the same procedure was adopted for these tests as for the smaller notched specimens. Crack depth usually was measured on three cross sections.

Data from these tests are listed in table IV. In view of the large size of these specimens and attendant costs of machining and testing, only a limited number of tests were run. From the table, however, it is seen that the most sharply notched specimens were cracked to an average depth of about 0.009 inch at a lifetime of only 500 cycles.

Information obtained from these tests is plotted on crack-depth—lifetime coordinates in figure 7. The triangles represent average crack depth for notched specimens ($K_t = 5.2$); the squares represent average crack depth for the more severely notched specimens.

The following comments are of interest:

- (1) The lifetime to form an observable crack is low. The tests demonstrate that cracks of appreciable depth (0.009 inch) are present at 500 cycles of 22.5-ksi stress. Cracks may have been present at an appreciably smaller number of cycles.
- (2) In the range of low to middle lifetime (<200,000 cycles), crack growth appears to be at a rate more rapid than for the small-diameter specimens. In this region, the crack depth around the circumference appears fairly constant.
- (3) At 22.5 ksi and for lifetimes in excess of 200,000 cycles, there appears to be a marked deceleration of crack growth. This is in the range of lifetime where acceleration of crack growth occurs for 1/4-inch-diameter specimens.
- (4) Crack propagation of large specimens notched with $K_t = 5.2$ and $K_t = 13.9$ appears the same. Note that all the data can be included within a narrow band.

DISCUSSION

References 1, 3, and 4 show, for small unnotched and mildly notched bars, that crack growth initially is slow and in later stages is rapid. In one of these investigations, (ref. 4) on 2024-T4 alloy, crack initiation required 40 to 90 percent of the lifetime of a mildly notched specimen, depending on stress level. The present investigation on severely notched bars of 2024-T4 alloy shows essentially the same crack-growth pattern. The major difference noted in this investigation was in earlier crack initiation. In these tests at 22.5 ksi, fatigue cracks were observed at less than 0.25 percent of the average lifetime to failure.

Early development of cracks also was observed in the large bars. In figure 7, bands are drawn of crack depth versus cycles showing differences in crack development for small- and large-diameter specimens. These differences in behavior noted in the figure, first in early stages and then at longer lifetimes, might result from a number of factors including (1) differences in residual stress at the notch root resulting from machining, (2) differences in the gross residual-stress picture resulting from heat treatment, (3) differences in stress gradient and other factors related to specimen size, and (4) others.

The experiment in which the behavior of a large bar having a polished notch was compared with that of a bar having an unpolished notch suggests that local stresses from machining may not be of major importance in these studies. This is in accord with DeForest's work (ref. 2) on SAE 1020 steel. He found that, although surface finish changed fatigue life at a given stress by a factor of 4, the growth of cracks was independent of surface state.

As described earlier, qualitative evidence of residual compressive stresses was found in the large bars. Such stresses might be expected to influence crack propagation. Small-bar behavior would be expected to be less influenced by such stresses, since residual stresses should be relieved when the small bars are sectioned from the large bars.

Evidence of a stress-gradient effect or of a size effect in crack growth is scarce. Moore (ref. 1) states that large bars (1-inch diameter) of railroad axle steel required a longer time from crack initiation to failure than did small bars (0.3-inch diameter) of the same steel. On the other hand, the smaller specimens lived longer at a given stress than did the larger bars. The data from this investigation are in accord with Moore's first observation but not with the second.

A number of investigators have attempted to develop expressions relating crack length to the number of cycles of repeated stress (see,

for example, refs. 3 and 7). If such expressions are applicable to the case of a severely notched bar, it can be shown that the rate of crack propagation is a function of the stress at the tip of the crack and the crack depth. Consideration was given to these various expressions with reference to the limited data available. However, explanation of the observation by means of such expressions seems unduly speculative at present. It would appear that further experimental information should precede extensive analysis.

Early crack initiation for notches with high values of Kt and factors influencing rates of crack propagation may be of considerable interest in airframe structures. However, it might be desirable first to explore whether another heat of 2024-T4 would show effects of the same nature and magnitude before making further detailed study of the present heat. With such further study, it should be possible to relate this behavior to residual stresses caused by extrusion and/or heat treatment (for example, by studying the behavior of large and small specimens from annealed bars).

If such experiments validated speculations considered in this investigation, further studies of crack initiation and propagation rate in relation to residual stresses resulting from extrusion and heat treatment may be desirable.

CONCLUDING REMARKS

In this investigation, V-notched bars of 2024-T4 aluminum alloy were tested in rotating-bending fatigue. Two sizes of specimens were involved, 1/4-inch-diameter and 2-inch-diameter specimens. The notches studied had severities of $K_t = 5.2$ and 13.9. A number of interesting observations were made during the course of the study related to crack initiation and crack propagation.

It appears that cracks initiated in severely notched bars earlier than in unnotched or mildly notched bars. Noticeably deep fatigue cracks were evident at 1,000 cycles or less at a stress level for which (in the case of 1/4-inch-diameter notched bars) failure might have been expected in the range 200,000 to 1,700,000 cycles. Propagation of these cracks appeared to be very slow for a major percentage of the lifetime. Acceleration of crack growth, shortly before failure, appeared to be associated with selected regions of the advancing crack front.

Differences in large-diameter and small-diameter specimen behavior were evident. These may have been associated with residual stresses which were shown qualitatively to be in the large bars.

It would appear that further exploration of this behavior should be made both experimentally and analytically to complement and extend the present knowledge of crack propagation.

Battelle Memorial Institute, Columbus, Ohio, July 29, 1955.

APPENDIX

ULTRASONIC TESTING OF 2024-T4 ALUMINUM-ALLOY BARS

Ultrasonic testing of bars of 2024-T4 aluminum alloy was considered necessary early in the investigation. In a previous investigation of notch-size effect on 7075-T6 alloy (ref. 8), considerable scatter in test results was encountered. Recent experiences in the aircraft industry (refs. 9 and 10) suggested that such scatter may result from metallurgical discontinuities such as inclusions and gas porosity. The ultrasonic inspection was carried out in an attempt to screen out bars containing such discontinuities.

Approximately 40 bars were examined. These were sectioned from 7 of the 11-foot round rods. Some of the bars were machined to a length of approximately 24 inches; others were machined to a 6-inch length. All bars had the ends carefully faced off by lathe-turning.

The first inspection was one of flaw detection. This was done with an ultrasonic Reflectoscope. The Reflectoscope is a pulse type of instrument that sends out a pulse of ultrasonic energy and receives a back reflection from any discontinuity such as the end of the bar or an inclusion or porosity. The bars were checked using the end-to-end technique at a frequency of 5 megacycles - the top frequency of the instrument. Flaws were discovered in seven bars, four from a round rod identified by the letter G and three from a round rod identified by the letter C. These bars also were checked on a special laboratory ultrasonic instrument at a frequency of 10 megacycles. This instrument is quite similar to the Reflectoscope. No additional flaws were discovered with this instrument.

Two of the bars lettered C were submitted to the metallographic laboratory for examination. The bar numbered C7 had a trace on the Reflectoscope screen as shown in figure 9. In this photograph, the vertical trace at the left represents the initial pulse; that at the right is the reflection at the end of the bar. The small blip near the initial pulse represents reflection from some discontinuity. Since the length between initial pulse and end reflection represented 24 inches on the bar, the distance to the discontinuity could be determined. Measurements of the appropriate distances on the film when converted to inches for the bar suggested the discontinuity to be 6.9 inches from the specimen end.

The bar was sectioned $6\frac{5}{8}$ inches from the end. It then was carefully polished. At a depth corresponding to about 6.7 inches, an inclusion

was found. The end view of the inclusion is shown magnified 100 times in figure 10(a). The specimen was remounted and polished from the side to determine the length of the inclusion. It was found to be about 3/32 inch in length. Figure 10(b) shows the side view of the inclusion at 45X.

Similar results were obtained on specimen C5. The inclusion found is observed in figure 11.

On the basis of these results, no specimens were used from rods lettered C and G, since inclusions appeared to string out along the length of the bar.

Other ultrasonic study included an investigation of attenuation properties of the bars. This was done by the back-echo decay method. When the sweep frequency of the Reflectoscope is adjusted so that all multiple back reflections are shown on the Reflectoscope, the back reflections present an exponential decay pattern. The number of back reflections may be related to fatigue behavior, but such a relationship may be difficult to ascertain.

Back-reflection decay patterns were recorded by photographing the cathode-ray tube screen. A set of five reflection patterns was taken on each bar at 5 megacycles. One of these was at the center of the bar; the other four were at 90° increments on a circle 1 inch from the axis of the bar.

Attenuation patterns obtained at the center of the bar could be placed in three categories based on the size of the first back reflection, that is, large, medium, and small, with the greater decrement associated with the larger initial reflection. With regard to attenuation patterns at the four outer positions, considerable variation was noted from bar to bar and also within the same bar. The cause for these variations may be geometric and metallurgical. The variations also may be influenced by the coupling of the ultrasonic transducer to the bar.

Some study of attenuation patterns was also carried out using a 10-megacycle excitation. The results were similar to those obtained with a lower frequency signal.

The results of the attenuation pattern did not directly influence the selection or rejection of any of the round bars. Of more importance to the program were the flaw-detection tests using ultrasonics. Such tests were useful in screening from the program material which may have provided undesirable variability in results.

REFERENCES

- 1. Moore, H. F.: A Study of Fatigue Cracks in Car Axles. Bull. No. 165, Eng. Exp. Station, Univ. of Ill., vol. 24, no. 41, June 14, 1927.
- 2. DeForest, A. V.: The Rate of Growth of Fatigue Cracks. Jour. Appl. Mech., vol. 3, no. 1, Mar. 1936, pp. A-23 A-25.
- 3. Bennett, J. A.: A Study of the Damaging Effect of Fatigue Stressing on X4130 Steel. Proc. A.S.T.M., vol. 46, 1946, pp. 693-711.
- 4. Bennett, J. A., and Weinberg, J. G.: Fatigue Notch Sensitivity of Some Aluminum Alloys. Res. Paper RP2495, Jour. Res., Nat. Bur. Standards, vol. 52, no. 5, May 1954, pp. 235-245.
- 5. Fenner, A. J., Owen, N. B., and Phillips, C. E.: The Fatigue Crack as a Stress-Raiser. Engineering, vol. 171, no. 4452, May 25, 1951, pp. 637-638.
- 6. Neuber, Heinz: Theory of Notch Stresses: Principles for Exact Stress Calculation. J. W. Edwards (Ann Arbor, Mich.), 1946.
- 7. Head, A. K.: The Growth of Fatigue Cracks. Rep. Met. 5, Aero. Res. Labs., Res. and Dev. Branch, Dept. Supply (Melbourne), July 1954.
- 8. Hyler, W. S., Lewis, R. A., and Grover, H. J.: Experimental Investigation of Notch-Size Effects on Rotating-Beam Fatigue Behavior of 75S-T6 Aluminum Alloy. NACA TN 3291, 1954.
- 9. Hitt, W. C.: Progress in the Field of Non-Destructive Testing Through the Use of Ultrasonics. Special Tech. Pub. No. 145, A.S.T.M., Nov. 1953, pp. 53-75.
- 10. Binsacca, A. P.: The Correlation of Ultrasonic Indications, Defects, and Metallurgical Properties in $2\frac{1}{2}$ Inch 75S Plate. Paper presented at Western States Convention of Society for Non-Destructive Testing, Mar. 30, 1955.

TABLE I

MECHANICAL PROPERTIES OF 2024-T4 ALUMINUM-ALLOY EXTRUDED ROD

Specimen (a)	Ultimate strength, ksi	Yield strength, 0.2-percent, ksi	Modulus of elasticity, ksi	Reduction in area, percent
A4 A4-2 B4 B4-2 C4 C4-2 D4-2 E4 E4-2 F4 F4-2 G4-2	71.3 65.0 73.2 66.7 72.5 65.6 73.0 65.7 71.7 65.1 74.0 66.4 73.1	49.0 46.0 51.3 44.3 50.5 43.7 50.3 46.0 49.0 44.5 51.0 46.0 51.0 45.5	9,600 10,450 10,550 10,320 10,450 10,000 10,800 10,550 10,220 10,450 10,450 11,500 10,450	13.6 16.4 12.2 14.4 14.2 14.2 11.8 15.3 13.5 15.6 12.0 15.7 11.8 15.7

aThe axes of the -2 specimens were 1 inch from the center of the 3-inch round rod, and the axes of the other specimens coincided with the axis of the 3-inch round rod.

TABLE II FATIGUE-TEST RESULTS ON 1/4-INCH-DIAMETER NOTCHED SPECIMENS

Specimen	Maximum nominal stress, ksi	Fatigue lifetime, cycles
	Unnotched spec	imens
^a D52-5A	50.0	19,000
D54-4A	50.0	20,000
D55-5A	40.0	153,000
D55-4A	40.0	167,000
		315,000
D52-3	35.0	310,000
D52-4	35.0	340,000
D54-5	35.0	354,000
D51-5A	35.0	417,000
D52-4A	35.0	440,000
D54-4	30.0	975,000
D56-5A	30.0	1,384,000
D52-3A	30.0	1,480,000
D54-5A	30.0	1,577,000
D51-5	30.0	10,225,000
D53-5	27.5	1,820,000
D53-5A	27.5	3,120,000
D51-4A	25.0	7,390,000
D56-5	25.0	9,983,000
D52-4A	22.5	b14,534,000
D51-5A	22.5	b15,000,000
	Notched specimens; K	t = 5.2
B61-4A	40.0	6,000
B63-2	40.0	19,000
B66-5A	35.0	17,000
B61-3A	35.0	19,000
B66-2	35.0	20,000
B63-3	35.0	60,000
B61-2	30.0	112,000
B63-5	30.0	160,000
aB61-2A	25.0	213,000
B63-2A	25.0	353,000
B64-3	25.0	367,000
B61-4	25.0	419,000
B64 -4	25.0	435,000
B66-3A	22.5	205,000
DOO-JA		333,000
P65 5		
B65-5	22.5	
B65-2	22.5	424,000
B65-2 B64-4A	22.5 22.5	1+24,000 1+74,000
B65-2 B64-4A B64-5	22.5 22.5 22.5	424,000 474,000 607,000
B65-2 B64-4A B64-5 B63-5A	22.5 22.5 22.5 20.0	424,000 474,000 607,000 3,595,000
B65-2 B64-4A B64-5	22.5 22.5 22.5	424,000 474,000 607,000 3,595,000 4,540,000
B65-2 B64-4A B64-5 B63-5A	22.5 22.5 22.5 20.0	424,000 474,000 607,000 3,595,000 4,540,000 b10,215,000
B65-2 B64-4A B64-5 B63-5A B61-5A	22.5 22.5 22.5 20.0 20.0	424,000 474,000 607,000 3,595,000 4,540,000
B65-2 B64-4A B64-5 B63-5A B61-5A B64-5A B64-2	22.5 22.5 22.5 20.0 20.0 20.0 20.0	424,000 474,000 607,000 3,595,000 4,540,000 b10,215,000 b10,795,000
B65-2 B64-4A B64-5 B63-5A B61-5A B64-5A	22.5 22.5 22.5 20.0 20.0 20.0	424,000 474,000 607,000 3,595,000 4,540,000 b10,215,000

These specimens were previously tested at lower stress levels and did not fail. bThese specimens did not fail.

TABLE III

CRACK-DEPTH MEASUREMENTS ON 1/4-INCH-DIAMETER NOTCHED SPECIMENS

							Average			
C	Maximum nominal	Duration of	Duration of Crack-depth measurements, in.		Crack-depth measurements, in.			in.	crack	
Specimen	stress, ksi	test, cycles	Section 1	Section 2	Section 3	Section 4	depth, in.			
B65-3A	35.0	1,000	0.0047	0.0053	0.0044		0.0048			
B62-4A	35.0	8,000	.0044	.0051	.0027	0.0018	.0035			
B62-2	35.0	10,000	.0134	.0177	.0196	.0133	.0160			
B64-3A	35.0	20,000		.0120		.0326	.0208			
B65-4	35.0	21,000	.0317	.0376	.0306	.0371	.0342			
B62-2A	35.0	50,000	.0510	.0370	.0379	.0502	.0425			
B64-2A	27.5	100,000	.0264	.0294	.0228	.0167	.0254			
B62-3A	27.5	150,000	.0431	.0255	.0244	.0418	.0330			
B65-4A	22.5	1,000	.0024		.0005	.0013	.0014			
B66-2A	22.5	10,000		.0013		.0024	.0018			
B65-2A	22.5	100,000	.0025	.0024	.0025	.0029	.0026			
B65-3	22.5	100,000	.0026	.0058	.0023	.0029	.0026			
B62-4	22.5	300,000	.0022	.0008	.0020	.0002	.0013			
B62-3	22.5	350,000	.0030	.0031	.0031	.0039	.0033			
B62-5A	22.5	350,000	.0025	.0455	.0504	.0022	.0251			
B66-3	22.5	610,000	.0023	.0030	.0028	.0028	.0026			
B66-4	22.5	626,000		.0025	.0033	.0031	.0030			
B66-4A	22.5	1,078,000	.0031	.0026	.0032	.0030	.0030			
B66-5	22.5	1,300,000	.0009	.0029	.0027	.0022	.0022			
B62-5	22.5	1,400,000	.0520	.0358	.0396	.0683	.0489			
B64-5A	20.0	10,215,000	.0046	.0049	.0031	.0025	.0038			
B64-2	20.0	10,795,000	.0031	.0068	.0031	.0038	.0042			

TABLE IV

FATIGUE DATA AND CRACK-DEPTH MEASUREMENTS ON 2-INCH-DIAMETER NOTCHED SPECIMENS

	Maximum	Duration	Develop	Crack-dep	oth measurem	ents, in.	Average crack
Specimen	stress, ksi	of test, cycles	Remarks	Section 1	Section 2	Section 3	depth, in.
Root radius, 0.016 inch; K _t = 5.2							
A5	32.5	79,000	Failed				
B2	22.5	4,947,000	Did not fail	0.044	0.040		0.042
D2	22.5	8,120,000	Cracked, did not fail				
D2	22.5	9,260,000	Remachined and polished, did not fail				
D2	27.5	679,000	Failed				
B5	22.5	8,015,000	Crack observed, 10,000 cycles				
В3	22.5	200,000	Test stopped	.036	.040	0.031	.036
E5	22.5	6,000	Test stopped	.028	.026		.027
Аб	15.0	14,828,500	Crack observed, 9,000 cycles, test stopped	.019	.014	.018	.017
		Roc	t radius, 0.002 i	nch; Kt = 1	-3.9		
E2	30.0	104,800	Failed		a		
F2	30.0	170,100	Failed				
A3	22.5	500	Test stopped	0.008	0.010	0.009	0.009
B7	22.5	3,000	Test stopped	.015	.017	.016	.016
D7	22.5	200,000	Test stopped		.030	.045	.038
D6	22.5	1,624,000	Test stopped	.045	.027		.036
D3	22.5	7,299,000	Test stopped	.031	.051		.041

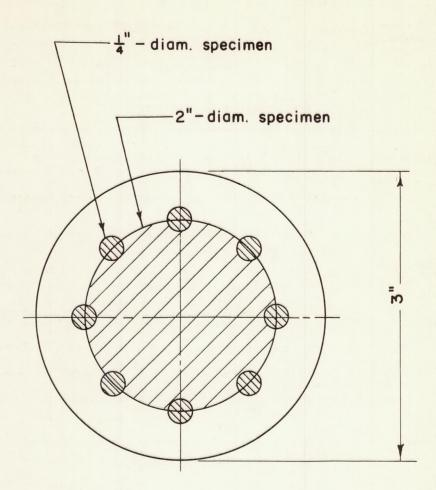
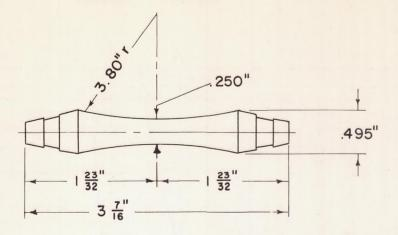
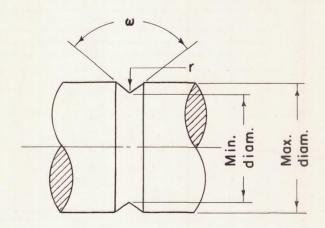


Figure 1.- Location of specimens in 3-inch-diameter round bars.



(a) 1/4-inch-diameter unnotched specimen.



Minimum diameter	Maximum diameter	r	deg
0.250	0.312	0.002	60
2.000	2.500	.016	60
2.000	2.500	.002	60

(b) Notched configuration (see table for dimensions).

Figure 2.- Unnotched and notched 1/4-inch-diameter specimens and notched 2-inch-diameter specimens

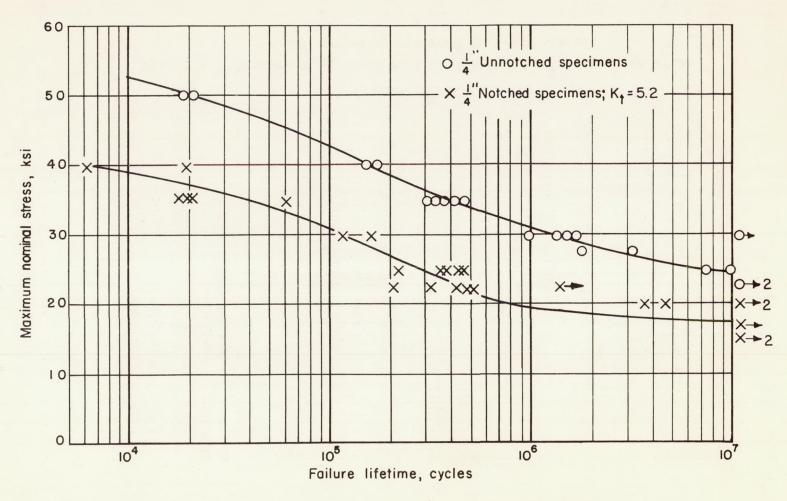
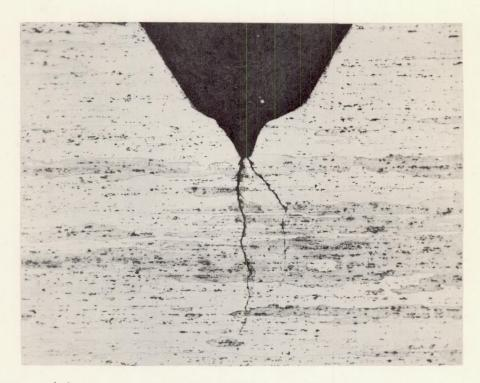


Figure 3.- Fatigue-test results on 1/4-inch-diameter specimens.



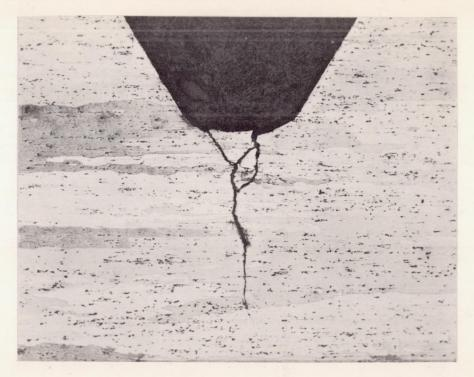
Figure 4.- Photograph of notch root of 2-inch-diameter specimen after 5×10^6 cycles of reversed 22.5-ksi stress.

NACA TN 3685



(a) Section showing cracks traversing notch root.

Figure 5.- Photomicrograph of notch root of 2-inch-diameter specimen after 5×10^6 cycles of reversed 22.5-ksi stress.



(b) Section showing crack propagation and separation of pieces of material.

Figure 5.- Concluded.

26 NACA TN 3685

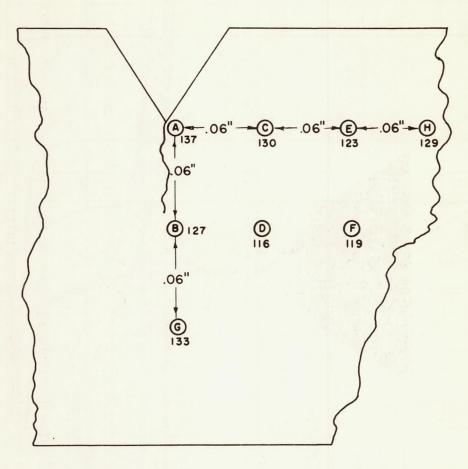


Figure 6.- Knoop hardness numbers on cross section of notched specimen shown in figure 4.

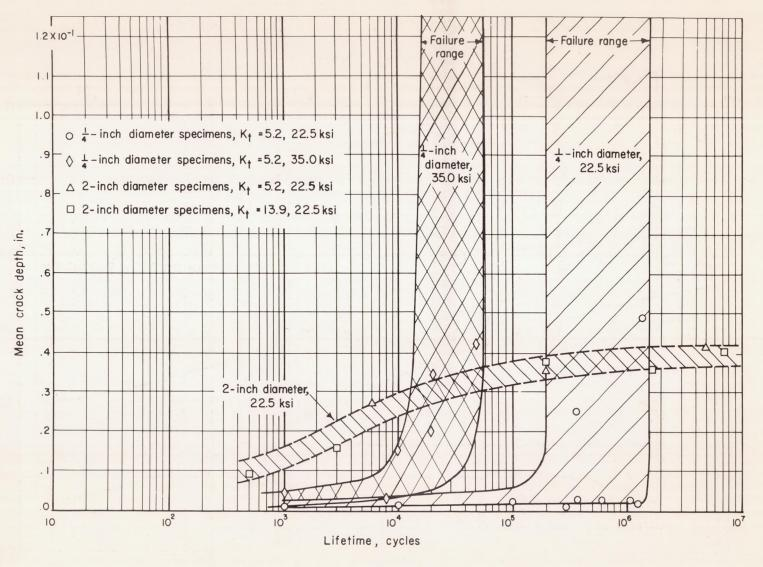


Figure 7.- Mean crack depth versus lifetime for severely notched specimens.

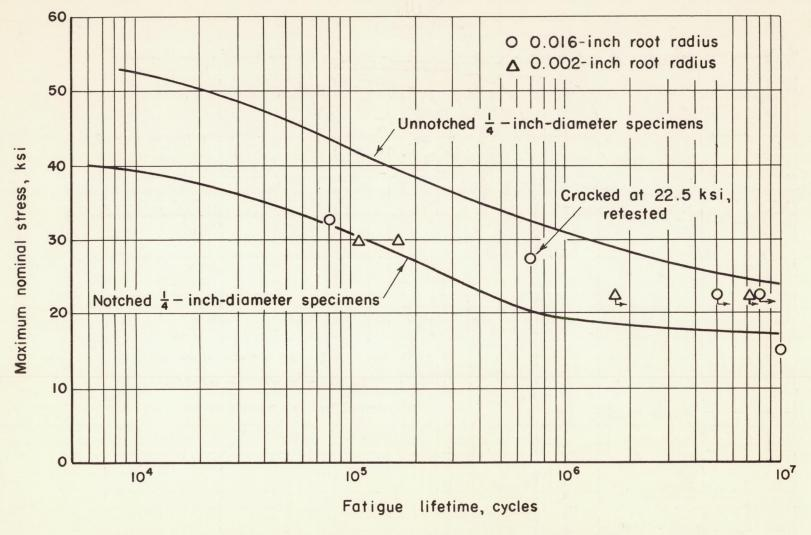


Figure 8.- Comparison of failure data obtained with large-diameter notched specimens with data from 1/4-inch-diameter specimens.

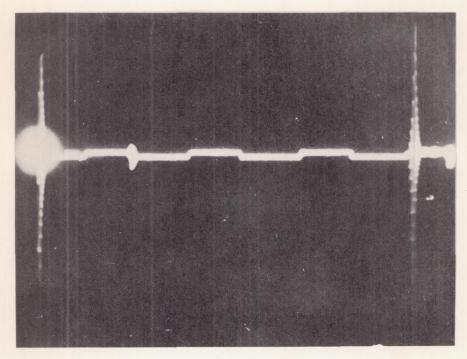


Figure 9.- Reflectoscope pattern of bar C7.

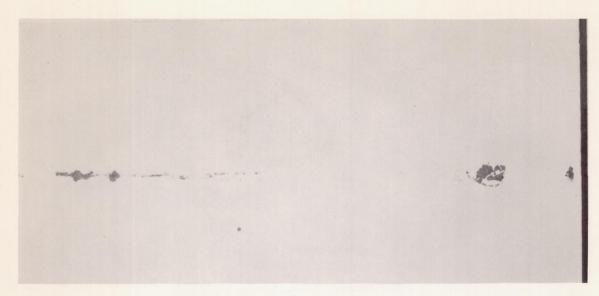


(a) End view of inclusion; 100X.

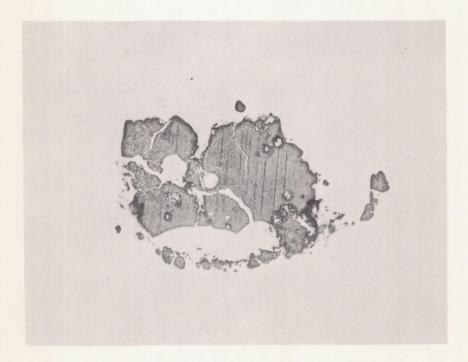


(b) Side view of inclusion; 45%.

Figure 10.- Inclusion found in bar C7.



(a) Side view of inclusion; 15X.



(b) Enlarged view of inclusion; 100X. Figure 11.- Inclusion found in bar C5.

